

# Circumstantial evidence for a non-Maxwellian plasma from femtosecond laser-matter interaction

Sachie Kimura and Aldo Bonasera

*INFN-LNS, via Santa Sofia, 62, 95123 Catania, Italy and  
Cyclotron Institute, Texas A&M University, College Station TX 77843-3366, USA*

(Dated: November 13, 2018)

We study ion acceleration mechanisms in laser-plasma interactions using neutron spectroscopy. We consider different types of ion-collision mechanisms in the plasma, which cause the angular anisotropy of the observed neutron spectra. These include the collisions between an ion in the plasma and an ion in the target, and the collisions between two ions in the hot plasma. By analyzing the proton spectra, we suggest that the laser-generated plasma consists of at least two components, one of which collectively accelerated and can also produce anisotropy in the angular distribution of fusion neutrons.

PACS numbers:

## I. INTRODUCTION

The development of small-scale high-intensity laser-systems with the chirped-pulse amplification (CPA) technique has opened new research fields of the laser-plasma interaction [1]. One of the promising applications of these studies is the ion-beam generation from laser irradiation on solid targets [2, 3, 4]. It is reported that protons in Mylar ( $\text{H}_8\text{C}_{10}\text{O}_4$ ) target irradiation are accelerated more effectively than in foil target irradiation. Understanding the ion acceleration mechanism in the laser-generated plasma is essential for applications. In this connection, nuclear reactions induced by laser-irradiation give a unique clue in understanding the ion-acceleration mechanism [5]. By replacing the protons in the plastic  $\text{CH}_n$  target by deuterons ( $\text{CD}_n$ ), a plasma of deuterium ions is generated. In the plasma the reaction  $\text{D}(d, n)^3\text{He}$  with a  $Q$ -value of 3.26 MeV is induced [6, 7, 8] and produces monochromatic neutrons. The angular distribution of the neutrons shows peculiar anisotropy not only on CD-plastic target [7, 8, 9] but also on  $\text{D}_2$ -gas jet [10] and on both  $\text{D}_2$  and  $\text{CD}_2$  clusters [11, 12]. The observed neutron angular distribution gives a direct hint to understand ion acceleration mechanisms in aneutronic reactions driven by laser as well [13, 14, 15].

In a recent paper [8], Habara et al. discuss the results of an experimental analysis of the neutron spectra in nuclear reactions induced by a laser-irradiation on a plastic CD target 50  $\mu\text{m}$  thick. They observed that neutron counts at  $I=1 \times 10^{19}$   $\text{W}/\text{cm}^2$  is larger and more anisotropic than that at  $I=2 \times 10^{18}$   $\text{W}/\text{cm}^2$ . This is attributed to the fact that higher intensity laser-pulse can accelerate ions more efficiently. The ion temperatures of 70 and 300 keV at  $I=2 \times 10^{18}$  and  $1 \times 10^{19}$   $\text{W}/\text{cm}^2$ , respectively, with a similar number of accelerated ions ( $N_i=10^{13}$ ) for both intensities are deduced, using a three-dimensional Monte Carlo (3D MC) code. They simulate ion acceleration processes under different assumptions and conclude that the deuterium ions are accelerated into the target and cause the nuclear reaction in the target. The directionality of the plasma beam is deduced from

the comparison to the differential cross section data of the reaction  $\text{D}(d, n)^3\text{He}$  in conventional laboratory beam-target experiments [16, 17, 18, 19, 20, 21]. In this paper we consider different types of ion-collision mechanisms in plasma, which cause the angular anisotropy of the observed neutron spectra, including collisions between an ion in the hot plasma and an ion in the target (HT), and collisions between two ions in the hot plasma (HH), using at first the total number of accelerated ions and the plasma temperature given in Ref. [8]. This assumption results in the overestimate of the absolute value of the neutron yield, if fusion for collisions between ions in the hot plasma are properly included. This component was ignored in Ref. [8]. Using the SRIM code [22] we estimate the HT component which suggests a smaller number of plasma ions compared to Ref. [8]. This, in turn, reduces the number of fusion originating from the collisions among hot ions in the plasma reconciling to the experimental observation. However, this is not the only possible explanation for the observed angular anisotropy in the neutron data. In fact the angular anisotropy in the neutron spectra can be observed, if a part of the plasma is collectively accelerated and even in the absence of HT mechanism. In order to shed some light on this point we study the plasma distribution reported in [3, 4] and show that indeed such a collective component is observed. We mention that the origin and the mechanism of accelerated ions have been discussed in detail, for a review Ref. [5, 23], and by now it is known the existence of at least two types of ion acceleration mechanisms, i.e., from the target front side into the target and from the target rear side to the vacuum. One of these mechanism becomes predominant depending on the target material and thickness or laser parameters. The later can be a candidate for the collectively accelerated plasma. Finally, we stress the importance of knowing both characteristics of fusion product, i.e., the spectra of neutron yield and the spectra of plasma ions, under common experimental conditions. At present those data are available only separately.

## II. NUMBER OF PLASMA IONS DERIVED FROM THE OBSERVED NEUTRON YIELD

In practice we consider the following two types of mechanisms for neutron generation in high intensity laser irradiation.

- (A) Collisions between two ions in the laser-heated plasma. Both ions are moving with thermal velocity. Under this assumption the direction of the incident reaction channel is random, hence the angular distribution of reaction products will be isotropic [7]. The contribution to the neutron yield from this mechanism is called ‘‘HH’’ in this paper.
- (B) Collisions between an accelerated ion in the laser-produced plasma and a cold nucleus in the bulk of the target. Under this second assumption the angular distribution of reaction products is possibly anisotropic. The contribution from this mechanism is called ‘‘HT’’ component.

We stress the importance of considering both mechanisms mentioned above, comprehensively, because either mechanism might be predominant, depending on the characteristics of the target. As an example in the case of neutron yield observation from laser pulses irradiation on deuterated clusters [12] both mechanisms play a key role.

If we assume that neutrons are produced by the collision of the ions in the hot plasma component (HH), in terms of the number of the accelerated ions  $N_i$ , the number of fusion per solid angle, or reaction rate [24], is given by

$$\frac{N_f^{(HH)}}{4\pi} = \frac{1}{4\pi} N_i n_{cr} \tau \int \sigma(v) v \phi(v) dv^3, \quad (1)$$

where  $n_{cr} = 10^{21}/\lambda^2$  is the plasma critical density [25, 26];  $\tau$  is the laser pulse duration;  $\sigma(v)$  and  $v$  are the reaction cross section and the relative velocity of the colliding ions. In general the reaction cross section  $\sigma(v)$  is given as a function of the incident energy, instead of the velocity, but here we have written it as a function of the velocity to keep the consistency in the velocity integral. Later  $\sigma$  will be represented as a function of the incident energy. We stress that assuming the critical density, which is the lowest limit to the real density reached in the experiment, the fusion yield given by Eq.(1) is underestimated. The density profile of the plasma simulated in Ref [8], using the PIC code, has an exponential shape which varies from  $4n_{cr}$  to  $0.1n_{cr}$ .  $\phi(v)$  is the relative velocity spectrum of a pair of ions and is given by a Maxwellian-distribution at the temperature  $kT_{HH} = 70$  or  $300$  keV:

$$\phi(v) = \left( \frac{\mu}{2\pi kT_{HH}} \right)^{\frac{3}{2}} \exp \left( -\frac{\mu v^2}{2kT_{HH}} \right), \quad (2)$$

where  $\mu$  is the reduced mass of ions. Eq. (1) gives  $1. \times 10^4$  and  $4. \times 10^4$ , per solid angle, at the temperature of 70

and of 300 keV, respectively, see Tab.I. The estimated yield is comparable with the neutron spectra in Figs 3 and 5 in Ref. [8]. The contribution from HH component is, therefore, expected to be seen in the figure as a peak at the neutron energy 2.45 MeV and to be isotropic [7]. In order to compare this to their energy distribution, we can roughly assume that the neutron distribution is a Gaussian distribution with a center-of-mass (CM) energy at 2.45 MeV and a width given by the temperature of the plasma. This gives an estimate at all angles of  $1.4 \times 10^5$  and  $1.3 \times 10^5$  ion/MeV/sr respectively, which is seen neither in figures 3 nor 5 in Ref. [8]. In the figures, if anything, one sees a clear angular dependence of the neutron yield and shifts of the observed peaks from the expected energy 2.45 MeV. This implies that either their estimated temperature or the number of accelerated ions given is too large. In other words the authors of Ref. [8] should have estimated the number of neutrons coming from the HH component, and show that this component is negligible compared to the HT contribution. As we will show in the following discussion, the contribution from the HT component, which has the correct angular dependence of the observed neutron spectra, is indeed dominant but with a smaller number of plasma ions.

If we consider the collisions between the ions in the plasma and the almost stable nuclei in the target (HT), the angular distribution of reaction products is expected to be anisotropic. To estimate the neutron yield from the HT component, one should take into account that one of the colliding ions is at rest in the laboratory frame. Therefore in the reaction rate per pair of colliding ions, the velocity spectrum Eq.(2) is modified as:

$$\phi_{HT}(v) = \left( \frac{m_1}{2\pi kT_{HH}} \right)^{\frac{3}{2}} \exp \left( -\frac{m_1 v^2}{2kT_{HH}} \right), \quad (3)$$

where  $m_1$  is the mass of ions in plasma, instead of the reduced mass. One can define an effective temperature as,

$$kT_{HT}^{eff} = (\mu/m_1)kT_{HH}. \quad (4)$$

Now we can use the effective temperature to estimate the number of fusion. For simplicity we estimate the most probable energy of the plasma ions that cause the nuclear reaction given by the Gamow peak energy ( $E_G$ ) [24]. The Gamow energy can be found using the saddle point method, i.e.:

$$\frac{d}{dE} \left( \frac{E}{kT} + bE^{-\frac{1}{2}} \right) = 0, \quad (5)$$

where  $b = 31.28Z_1Z_2M^{\frac{1}{2}}$  (keV $^{\frac{1}{2}}$ ), denoting the atomic number of the colliding nuclei  $Z_1, Z_2$  and the reduced mass number  $M$ . We remind that  $M = A_1A_2/(A_1 + A_2)$ , where  $A_1$  and  $A_2$  are the mass numbers of the colliding ions, respectively, is different from the reduced mass  $\mu$ . The temperature  $kT$  is replaced by the plasma temperature, i.e., the temperature of the HH component in conventional discussions, but for the present case of the HT

component,  $kT$  is replaced by the effective temperature. Then,

$$E_G = \left( bkT_{HT}^{eff}/2 \right)^{\frac{2}{3}}. \quad (6)$$

We specially mention that Eq. (5) is valid in the case of sub-barrier reactions, because this condition comes from the product of a Maxwellian and the Coulomb barrier penetrability [24]. The height of the Coulomb barrier for the reaction  $D(d, n)^3\text{He}$  is estimated to be about 470 keV. By approximating the energy of the accelerated ions by the Gamow energy Eq. (6), the neutron yield per solid angle is written as:

$$\frac{N_f^{(HT)}}{4\pi} = \frac{1}{4\pi} N_i \sigma(E_G) n_T d, \quad (7)$$

where  $\sigma(E_G)$  is the reaction cross section at the Gamow energy. The reaction cross section data at this energy are taken from NACRE compilation [27] and given in Table I. The number density of the solid polyethylene target:  $n_T = 1.2 \times 10^{23}$  atoms/cm<sup>3</sup> and  $d$  is the projected range [22] of the accelerated ions in the target. Using the above listed numbers the neutron yield per solid angle is also reported in Tab. I. As a consequence of this simple estimate, the yield per solid angle under this assumption is a factor  $10^2$  higher than the yield from the collisions between two ions in the plasma. This is because the number density of the solid target is much higher than that of the laser-generated plasma. However from eq. (4) the effective HT temperature is lower than the HH one, depending on the asymmetry in mass of the fusion ions. The higher temperature in the HH collision mechanism has an advantage of the higher fusion cross section. There is, therefore, a competition between two mechanism depending on the laser-intensity. This feature might explain why at lower intensities (i.e. lower T) the neutron angular distribution is less anisotropic: At the lower intensity irradiation, the contribution from the HT component to the neutron yield is suppressed compared with the higher intensity irradiation. In fact the temperature of the HT component is low and most reactions happen below the Coulomb barrier. The nuclear reactions below the barrier are exponentially suppressed. Therefore the HH mechanism, which has higher temperature, contributes to the less anisotropic neutron yield angular distribution. On the other hand, if the plasma temperature is high enough, the corresponding Gamow energy is above the Coulomb barrier. At energies above the Coulomb barrier, i.e. high T, to have higher densities gives higher fusion probabilities (above the barrier fusion probabilities depend quadratically on densities and do not depend much on T) thus collisions between an ion from the plasma and an ion from the target becomes more probable. We expect that in some temperature region there is a transition from collisions occurring mainly in the plasma to collisions occurring between the plasma ions and the target ones. An experimental detailed investigation of this transition region would be very interesting

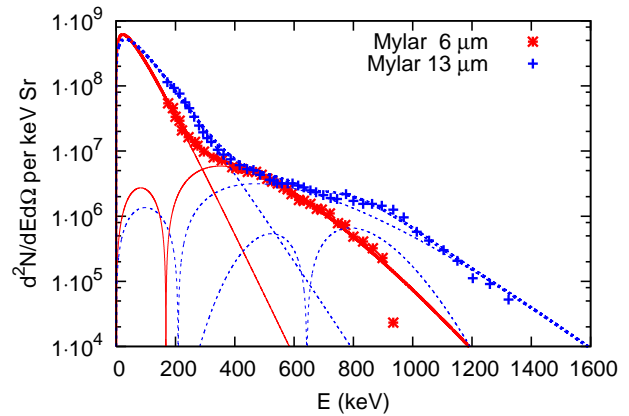


FIG. 1: Experimental data of proton energy spectra for Mylar targets 6 (asterisks) and 13 (crosses)  $\mu\text{m}$ -thick retrieved from Lee et al. [4]. The thick curves represent fitting of the proton spectra using Maxwellian distributions and distributions with extra accelerations. The thin curves are the different components and are summed into the thick curves. The obtained fitting parameters are given in Tab. II.

and instructive in order to understand the microscopic dynamics of fusion.

The HT contribution to the neutron yield is a factor  $10^2$  higher than experimentally observed data [8], as well. This again implies that either the estimated temperatures are too high or the estimated number of ions in the plasma is too large. From this simple estimate and the one above from the HH component we can argue that the number of ions in the plasma could be at least two orders of magnitude smaller than that estimated in Ref. [8], i.e., about  $10^{11}$ , instead of  $10^{13}$ . This reduction of the number of accelerated ions results in a suppression of the neutron yield from the HH component which becomes negligible. A more involved calculation solving eq.(1) for the HT component numerically gives results in agreement with our simple estimate and will be discussed in more detail in a following paper [28].

### III. PLASMA TEMPERATURE SUGGESTED BY THE PROTON SPECTRA FROM PLASTIC TARGETS IRRADIATION

Another evidence of the smaller number of plasma ions is shown by a direct observation of proton spectra in laser irradiation [3, 4]. Fig. 1 in Lee et al. [4] shows the proton energy distribution at the laser intensity  $I = 2.2 \times 10^{18}$  W/cm<sup>2</sup> similar to [8], and the target material is Mylar or aluminum. We are especially interested in the results from the Mylar target, because the characteristics of the produced plasma should be close to the characteristics of the plasma from the deuterated plastic targets. We, therefore, selected two results from 6 and 13  $\mu\text{m}$  thick Mylar target. A peculiar feature of the proton energy distribution is that it exhibits bumps in the higher energy

TABLE I: Plasma temperature ( $kT_{HH}$ ) and neutron yield per solid angle ( $N_f^{(HH)}/Sr$ ) from the HH component and the effective temperature ( $kT_{HT}^{eff}$ ) and  $N_f^{(HT)}/Sr$  from the HT component at the given laser intensities.

I (W/cm <sup>2</sup> )	$kT_{HH}$ (keV)	$N_f^{(HH)}/Sr$	$kT_{HT}^{eff}$ (keV)	$E_G$ (keV)	$\sigma(E_G)(10^{-27}\text{cm}^2)$	$d(\mu\text{m})$	$N_f^{(HT)}/Sr$
$2 \times 10^{18}$	70	$1. \times 10^4$	35	67	24	0.8	$4. \times 10^9$
$1 \times 10^{19}$	300	$4. \times 10^4$	150	176	66	2.	$3. \times 10^6$

TABLE II: Fitting parameters for proton energy spectra from 6 and 13  $\mu\text{m}$  thick targets irradiation. Especially for 13  $\mu\text{m}$  thick target we have used three components, two of which have different relative velocities with respect to the hot-plasma component.

T thick. ( $\mu\text{m}$ )	$c$ ( $10^{11}$ )	$kT_{HH}$ (keV)	$c_1$	$kT_1$ (keV)	$E_0$ (keV)
6	$(3.0 \pm 0.2)$	$44. \pm 1.$	$(3.5 \pm 0.7) 10^9$	$52. \pm 5.$	$170. \pm 20.$
13	$(3.5 \pm 0.1)$	$61. \pm 1.$	$(3. \pm 2.) 10^9$ $(4. \pm 1.) 10^7$	$78. \pm 30.$ $14. \pm 5.$	$210. \pm 60$ $695. \pm 10$

region. This feature could be attributed to the existence of at least two different components in the plasma. To describe these characteristics, we use a Maxwellian distribution in terms of the energy of the protons in the lab. system ( $E$ ):

$$\frac{d^2 N}{dE d\Omega} = c \frac{1}{2\sqrt{\pi^3}} \frac{\sqrt{E}}{(kT_{HH})^{3/2}} \exp(-E/kT_{HH}). \quad (8)$$

To this we add a Maxwellian distribution of a moving source [29]:

$$\frac{d^2 N}{dE d\Omega} = \frac{c_1}{4\pi} \frac{\sqrt{EE'}}{(kT_1)^2} \exp(-E'/kT_1), \quad (9)$$

where  $E' = E - 2\sqrt{EE_0} + E_0$ . Both equations are normalized to  $1/4\pi$ . The latter gives a part of the plasma in translational motion with respect to the laboratory system with a collective kinetic energy  $E_0$ . The obtained fitting curves are shown by thick solid and dashed curves for the spectra at 6 and 13  $\mu\text{m}$  thick targets irradiation, respectively, in Fig. 1. The thin curves show each component which add into the thick curves. Especially for the spectra at 13  $\mu\text{m}$  thick target, we have used a sum of three components, two of them have different extra acceleration energies  $E_0$ . The corresponding fitting parameters are summarized in Tab. II. From the fitting we can deduce the number of ions in the plasma  $N_i \sim 3 \times 10^{11}$  and the plasma temperature of  $kT_{HH} \sim 44$  and  $61$  keV for 6 and 13  $\mu\text{m}$  thick targets, respectively. The deduced number of plasma ions is in agreement with our yield estimation from the neutron measurement. Moreover one can see clearly that the proton spectra differ from a Maxwellian but a part of plasma is accelerated to higher energy with  $E_0$ . Similar features of the proton spectra in laser-produced plasma can be found in Spencer et al. [3], as well. The possible reasons for such

a collective acceleration will be discussed in a following publication [28].

In Fig. 7 and 8 of [8], the authors discuss the ratio of the neutron yields at the angle of  $23^\circ$  to that at the angle of  $67^\circ$  from the target rear normal. They found that the ratio can be larger than 3. In Fig. 2 the ratio of the differential cross sections in beam-target experiments [16, 17, 18, 19, 20, 21] at laboratory angles  $23^\circ$  to  $67^\circ$  is shown by thick curves. There is a discrepancy between [sc72] data [18] and [li73] [19] in the energy region higher than 3 MeV. Nevertheless the figure shows clearly that the ratio can, indeed, be larger than 3 and less than 3.5 at the incident deuteron energy  $E_L$  from 1.75 to 1.96 MeV. Thus the accelerated deuterons which contribute to the nuclear reactions have energies slightly less than 2 MeV. In the CM frame  $E \sim 0.9$  MeV, i.e., the corresponding Gamow peak energy is about 900 keV. If we use  $E_G = 900$  keV, the neutron yield per solid angle from the HT collision is estimated to be of the order of  $10^7$  from Eq. (7), adopting the number of accelerated ions given in [8]. This number is 10 times higher than that in Table I. In other words, to reproduce the experimental data, one needs to assume  $N_i \sim 10^{10}$ , as the number of accelerated ions in plasma. In passing we note that the ratio of the neutron yield taken at the angle of  $20^\circ$  to that of  $85^\circ$  is higher than the previous one as shown in Fig. 2 by thin curves with smaller points. A careful experimental determination of this feature would be very useful.

We can also derive the plasma temperature corresponding to  $E_G = 900$  keV. Since at this energy we are above the Coulomb barrier, we can estimate it from the classical relation:

$$E_G = (3/2)kT_{HH}, \quad (10)$$

which gives  $kT_{HH} = 600$  keV, i.e., higher than the estimated temperature in Ref. [8]. This contradiction might be solved by considering that a part of the plasma deuterons is collectively accelerated at energy  $E_0$ , as we have shown in the analysis of proton spectra. This extra acceleration energy can reach about 700 keV which is close to 900 keV. In the presence of an extra acceleration, the plasma temperature cannot be derived simply from the relation (10). The difference between the plasma temperature deduced from the ratio at two angles and the one estimated by Ref. [8] suggests that the plasma spectra is different from a usual Maxwellian distribution. In other words, the difference justifies the presence of the collective motion of a part of the plasma. Indeed the col-

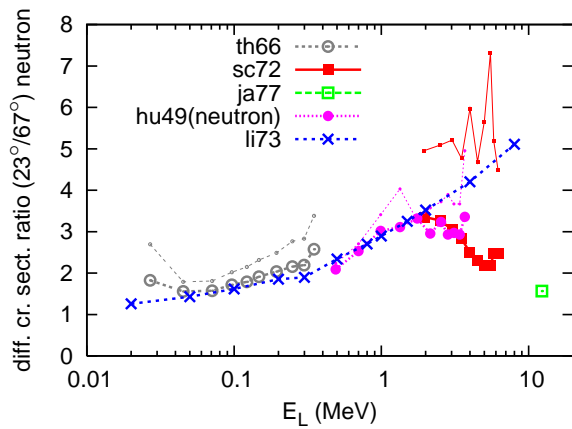


FIG. 2: The ratio of differential cross sections at two angles. The ratio at angles  $23^\circ$  to  $67^\circ$  is shown by large points connected by curves, while the ratio at angles  $20^\circ$  to  $85^\circ$  is shown by smaller points connected by thin curves, for a comparison. The experimental data are retrieved from EXFOR-data system [30]. hu49-data (pink filled circles) are evaluated from the angular distribution of the DD neutron yield [16] and the others, th66-data (grey open circles) [17], sc72 (red filled squares) [18], ja77 (green open squares) [20] and li73 (blue crosses) [19], are converted from the  $^3\text{He}$  angular distribution of the DD reaction.

lisions between two ions in the plasma which is moving at a collective energy  $E_0$  in the laboratory frame can result

in the angular anisotropy of the neutron yield. This is a possible mechanism to explain the angular anisotropy experimentally observed.

#### IV. CONCLUSIONS

In conclusion, we have discussed different possible ion-collision mechanisms, which can result in the observed anisotropic neutron spectra. When analyzing the proton spectra, we have found that there are at least two plasma components: one is approximated by a Maxwellian distribution and the other has a collective motion relative to the former component. Comparing the ratios in the neutron counts at two angles in the experiment to the differential cross sections measured in conventional beam-target experiments, the most effective energy is estimated to be 0.9 MeV with corresponding plasma temperature of 600 keV, which is higher than the estimated plasma temperature in Ref. [8]. We have discussed a possible solution of this contradiction, in connection with the collective motion of a part of the plasma, which can in principle explain the observed neutron angular anisotropy. We suggest that an experimental determination of the neutron angular anisotropy in coincidence with the plasma distribution would be very interesting and give useful information on the mechanisms at play.

- 
- [1] K. Ledingham, P. McKenna, and R. Singhal, *Science* **300**, 1107 (2003).
  - [2] A. J. Mackinnon, Y. Sentoku, P. K. Patel, D. W. Price, S. Hatchett, M. H. Key, C. Andersen, R. Snavely, and R. R. Freeman, *Phys. Rev. Lett.* **88**, 215006 (2002).
  - [3] I. Spencer, K. W. D. Ledingham, P. McKenna, T. McCanny, R. P. Singhal, P. S. Foster, D. Neely, A. J. Langley, E. J. Divall, C. J. Hooker, et al., *Phys. Rev. E* **67**, 046402 (2003).
  - [4] K. Lee, S. H. Park, Y.-H. Cha, J. Y. Lee, Y. W. Lee, K.-H. Yea, and Y. U. Jeong, *Phys. Rev. E* **78**, 056403 (2008).
  - [5] S. Karsch, S. Düsterer, H. Schwoerer, F. Ewald, D. Habs, M. Hegelich, G. Pretzler, A. Pukhov, K. Witte, and R. Sauerbrey, *Phys. Rev. Lett.* **91**, 015001 (2003).
  - [6] P. A. Norreys, A. P. Fews, F. N. Beg, A. R. Bell, A. E. Dangor, P. Lee, M. B. Nelson, H. Schmidt, M. Tatarakis, and M. D. Cable, *Plasma Phys. Control. Fusion* **40**, 175 (1998).
  - [7] N. Izumi, Y. Sentoku, H. Habara, K. Takahashi, F. Ohtani, T. Sonomoto, R. Kodama, T. Norimatsu, H. Fujita, Y. Kitagawa, et al., *Phys. Rev. E* **65**, 036413 (2002).
  - [8] H. Habara, R. Kodama, Y. Sentoku, N. Izumi, Y. Kitagawa, K. A. Tanaka, K. Mima, and T. Yamanaka, *Phys. Rev. E* **69**, 036407 (2004).
  - [9] D. Hilscher, O. Berndt, M. Enke, U. Jahnke, P. V. Nickles, H. Ruhl, and W. Sandner, *Phys. Rev. E* **64**, 016414 (2001).
  - [10] S. Fritzler, Z. Najmudin, V. Malka, K. Krushelnick, C. Marle, B. Walton, M. S. Wei, R. J. Clarke, and A. E. Dangor, *Phys. Rev. Lett.* **89**, 165004 (2002).
  - [11] T. Ditmire, J. Zweiback, V. Yanovsky, T. Cowan, G. Hays, and K. Wharton, *Nature* **398**, 489 (1999).
  - [12] F. Buergens, K. W. Madison, D. R. Symes, R. Hartke, J. Osterhoff, W. Grigsby, G. Dyer, and T. Ditmire, *Phys. Rev. E* **74**, 016403 (2006).
  - [13] V. S. Belyaev, A. P. Matafonov, V. I. Vinogradov, V. P. Krainov, V. S. Lisitsa, A. S. Roussetski, G. N. Ignatyev, and V. P. Andrianov, *Phys. Rev. E* **72**, 026406 (2005).
  - [14] S. Kimura, A. Anzalone, and A. Bonasera, *Phys. Rev. E* **79**, 038401 (2009).
  - [15] A. Bonasera, A. Caruso, C. Strangio, M. Aglione, A. Anzalone, S. Kimura, D. Leanza, A. Spitaleri, G. Imme, D. Morelli, et al., *Fission and properties of neutron-rich nuclei - Proceedings of the Fourth International Conference* p. 503 (2008).
  - [16] G. Hunter and H. Richards, *Phys. Rev.* **76**, 1445 (1949).
  - [17] R.B.Theus, W.I.McGarry, and L.A.Beach, *Nucl. Phys.* **80**, 273 (1966).
  - [18] R. Schulte, M. Cosack, A. Obst, and J. Weil, *Nucl. Phys. A* **192**, 609 (1972).
  - [19] H. Liskinen and A. Paulsen, *Nuclear Data Tables (Nuclear Data Sect.A)* **11**, 569 (1973).
  - [20] J. N. Jarmie, *Phys. Rev. C* **16**, 15 (1977).
  - [21] R. E. Brown and N. Jarmie, *Phys. Rev. C* **41**, 1391 (2001).

- (1990).
- [22] J. Ziegler, URL <http://www.srim.org/>.
- [23] J. Fuchs, Y. Sentoku, E. d'Humieres, T. E. Cowan, J. Cobble, P. Audebert, A. Kemp, A. Nikroo, P. Antici, E. Brambrink, et al., *Physics of plasmas* **14**, 053105 (2007).
- [24] D. D. Clayton, *Principles of Stellar Evolution and Nucleosynthesis* (University of Chicago Press, 1983).
- [25] D. W. Forslund, J. M. Kindel, and K. Lee, *Phys. Rev. Lett.* **39**, 284 (1977).
- [26] F. Begay and D. W. Forslund, *Phys. Fluids* **25**, 1675 (1982).
- [27] C. Angulo, M. Arnould, M. Rayet, P. Descouvemont, D. Baye, C. Leclercq-Willain, A. Coc, S. Barhoumi, P. Aguer, C. Rolfs, et al., *Nucl. Phys. A* **656**, 3 (1999).
- [28] S. Kimura and A. Bonasera, to be submitted.
- [29] T. C. Awes, G. Poggi, C. K. Gelbke, B. B. Back, B. G. Glagola, H. Breuer, and V. E. Viola, *Phys. Rev. C* **24**, 89 (1981).
- [30] URL <http://www-nds.iaea.org/exfor/exfor.htm>.